

A miniature turn-around for distributed temperature sensing

Xiaoguang Sun, David T. Burgess, Kyle Bedard, Jie Li and Mike Hines
OFS, 55 Darling Drive, Avon, CT 06001

Copyright 2015 Society of Photo-Optical Instrumentation Engineers.

ABSTRACT

In many fiber optic distributed temperature sensing (DTS) systems, a dual-ended configuration can correct the temperature measurement error associated with wavelength dependent loss (WDL) of the optical fiber and can provide a more accurate temperature measurement in comparison with a single-ended fiber system. In this configuration, two pieces of fiber are laid parallel to each other and connected at the distal end by a turn-around device, creating a U-shaped optical path that provides accessibility to both legs from the proximal end of the system. In many applications, tightly confined spaces constrain the fiber bend diameter and thus the size of the turn-around device. In this paper we will report a miniature turn-around built with a short section of a graded index (GI) fiber. The device measures less than 300 μm in diameter and less than 2 mm in length. The insertion loss of the miniature turn-around is measured and will be compared with the theoretical simulations.

Keywords: distributed sensing, optical fiber, multicore, Raman, DTS

1. INTRODUCTION

Raman scattering based distributed temperature sensing (RDTS) using optical fibers has been widely used in a variety of applications since it was first demonstrated some thirty years ago [1]. RDTS systems can achieve long sensing range, short spatial resolutions on the order of 1 meter, and temperature sensitivity around 0.1K, all at a very low cost compared to other alternate distributed sensing methods.

The RDTS system is based on Raman optical time-domain-reflectometry (OTDR) measurements: when laser light is coupled into the fiber, a small fraction of the input light is scattered due to Rayleigh, Brillouin and Raman scattering. The scattered light travels in reverse to the input end and from the time of flight, the location of the scattering in the fiber can be precisely calculated. The scattered Raman light has two components: anti-Stokes (AS), which has a shorter wavelength than that of the incident light (blue-shifted), and Stokes, which has a longer wavelength (red-shifted). The intensity of the AS light is more temperature sensitive than that of the Stokes light, thus by measuring the intensity ratio of the back-scattered AS to Stokes light, the temperature along the fiber can be measured. But the measured ratio at the optical detector also depends on the loss experienced by the AS and Stokes light traveling back from the scattering site. Since the wavelength difference between the AS and Stokes light can be more than 100 nm, the loss difference can be large over a long distance, and can introduce errors in the measured temperature. This wavelength dependent loss (WDL) can be caused by Rayleigh scattering within the fiber, fiber splices, connectors, stress on the optical fiber and hydrogen or radiation induced loss in the optical fiber. The WDL induced temperature error can be several degrees, which may not be acceptable.

Several methods have been proposed and applied to solve the temperature error associated with the WDL. For example, such methods include: two light sources with a wavelength difference equal to the wavelength shift of the AS light [2]; a high reflection mirror at the far end of the fiber [3], and dual-ended systems [4]. All of these methods have advantages and disadvantages; for example, the first approach requires two light sources, and the spectrum of the scattered of AS and Stokes light may differ from those of the launched light, causing difficulty in correcting the WDL. The dual-ended systems have attracted more interest since they are more robust and can automatically correct the WDL, the downside being that they require an optical sensing length two times that of single-ended approaches.

In typical dual-ended systems, two individual optical fibers are laid parallel to each other and are connected at the distal end so light can be coupled into either leg at the proximal end for injection and detection of Raman signals. The connection at the distal end can be done by bending a short length of fiber (miniature bend) and splicing the two lengths

of single-core sensing fibers together, creating a single, U-shaped optical path. Aside from the optical loss induced by the tightly bent fiber, the strain associated with such a tightly bent fiber bend could limit the life time of the turn-around. The reliability of the bent fiber is a critical consideration in some applications, where limited installation space will restrict the extent to which the fiber can be bent, particularly in harsh environments like high temperature and high humidity. The effects of bending might be mitigated by using a smaller cladding size and/or annealing of the fiber and encapsulating the bent section of the fiber in a sealed compartment; however, the final device is typically bulky and the integrity of the fiber somewhat compromised.

In this paper we will demonstrate a miniature turn-around using a dual-core sensor fiber spliced to a segment of graded index (GI) fiber lens. The turn-around has a diameter less than 300 μm and length less than 2 mm. It has very low loss at the intended operating wavelength. Since the device is not under any bend stress its reliability is greatly improved. Key properties of the dual-core fiber including geometry, attenuation, and crosstalk will also be described in the paper.

2. EXPERIMENT

2.1. Dual-core fiber

The end-face image of the dual-core fiber is shown in Figure 1. The dual-core fiber has two 50 μm diameter GI multimode (MM) cores spaced 100 μm apart and the numerical aperture (NA) of the MM cores is 0.20. The MM cores are optically compatible with commonly available single-core 50/125 GI fiber typically used in DTS systems. The outer glass cladding diameter is 200 μm , allowing greater separation between the cores to minimize crosstalk. The large spacing between the cores also simplifies the connection of individual single-core fibers to the cores of the dual-core fiber, facilitating connection to commercially available interrogator equipment. The fiber is coated with a 350 μm diameter dual Acrylate coating. To connect between the dual-core structure and independent single-core fibers, fan-outs were made with commercially available GI 50/125 fibers and the dual-core sensor fiber. The fan out has an insertion loss of <0.5dB from 850nm to 1300 nm, and a crosstalk <-60dB. The dual-core end of the fan-out can be spliced to the dual-core fiber using a polarization maintaining (PM) fiber splicer, and the splicing loss of the two cores is typically <0.1dB.

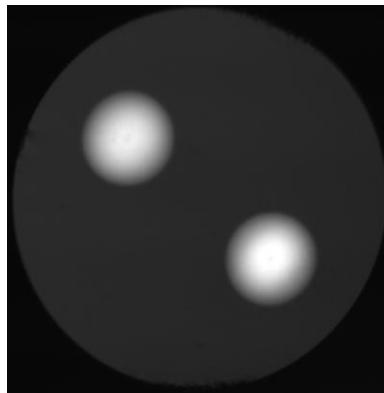


Figure 1. End-face image of the dual-core fiber taken by an optical microscope with the fiber illuminated from bothends

The spectral attenuation of the dual-core fiber was measured by the cutback method using a PK2500 optical bench with a fan-out spliced to the dual-core fiber and is shown in Figure 2. The loss is similar to those of commercially available single-core 50/125 μm GI fibers. The loss is about 1.2 dB/km around 1064 nm, and the loss peak at 1385 nm is <0.5dB.

Low optical crosstalk between the two cores is important for the dual-core fiber to be used in the distributed sensing applications as high crosstalk could create error in the temperature measurement. Crosstalk between the cores is related to the distance between the cores, core diameter variation and scattering, etc. Bend can also induce core-to-core crosstalk; hence we measured the crosstalk vs. bend diameter using a 2-point bend device. A 2.63km long dual-core fiber was coiled on a 10-inch spool with fan-outs spliced to both ends of the fiber. 1064nm light was launched into one core at one end and the power from both cores was measured at the output end. The crosstalk is defined as $crosstalk = 10 \cdot \log(P2 / P1)$ where $P1$ is the power from the core the light was launched into, and $P2$ is from the other.

A section of the dual-core fiber near the output end was put into a 2-point bend device to bend the fiber 180 degrees. The

fiber was rotated to create maximum (worst case) crosstalk. The total crosstalk of the 2.63km system, including the two fan-outs, was -58dB when the bend diameter was over 60mm. From Figure 3, we can see that the crosstalk can be less than -50dB with diameters larger than 35mm.

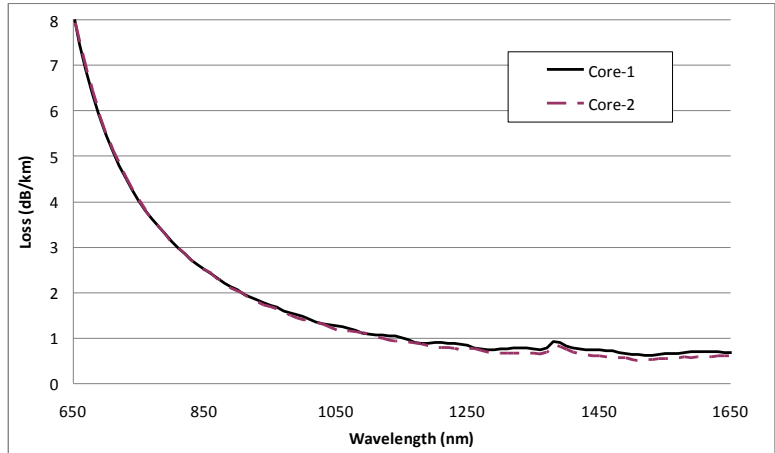


Figure 2. Spectral attenuation of dual-core fiber measured by the cutback method.

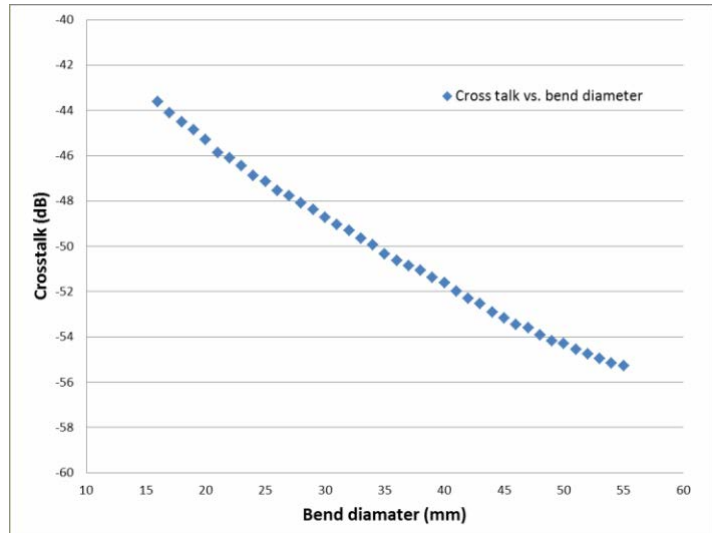


Figure 3. Crosstalk vs. bend diameter at 1064nm

2.2. Turn-around

An illustration of the turn-around is shown in Figure 4. The left side represents the dual-core fiber while the right side represents a GI fiber with a high reflectance coating applied to its end face. The cladding diameter of the GI fiber lens in our experiment is 200 μm to match that of the dual-core fiber.

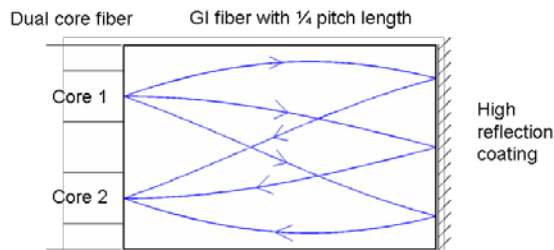


Figure 4. Illustration of dual-core fiber turn-around.

The index distribution of the GI fiber lens can be described as [5]:

$$n(r) = n_0 \left(1 - \frac{g^2}{2} r^2 \right) \quad (1)$$

where r is radial distance from the center, n_0 is refractive index at the center of the GRIN fiber, and g is the gradient. The gradient g is related to the measured NA and the core size a by:

$$g = \frac{NA}{a \cdot n_0} \quad (2)$$

A beam propagating in the GI medium follows a sinusoidal path, and the pitch or period of the sinusoidal path [5] is:

$$P = 2\pi/g \quad (3)$$

So, if we place a high reflection mirror at the $\frac{1}{4}$ pitch position, then the input will be mirrored to its opposing side (opposite core) with a 1:1 ratio. We illustrate this in Figure 4: the light exiting from Core-1 will expand and be collimated by the GI fiber, then will be reflected by the mirror and focused into Core-2. In this experiment, the core diameter of the GI fiber is $180 \mu\text{m}$ and the NA is 0.275; the calculated length of the $\frac{1}{4}$ pitch is $\sim 757 \mu\text{m}$ by equation (3). Therefore the entire device can be miniaturized in diameter and length, while reducing its complexity and creating a more robust turn-around.

The coupling efficiency of the turn-around depends on the length of the GI fiber, the angle of the GI fiber end face, and the offset of Core 2 to the ideal location, and this efficiency can be numerically calculated [6]. The coupling loss vs. the GI fiber length, the end face angle, and the offset of Core 2 is plotted in Figure 5. From the plots we can see that in order to achieve a loss of < 0.5 dB we need to control the deviation of the GI fiber length to less than $4 \mu\text{m}$, the GI fiber end face angle to less than 0.5 degree, and the offset of Core 2 to less than $3 \mu\text{m}$. The GI fiber length and the end face angle depend on the fiber cleaver and are achievable with commercially available equipment. The offset of Core 2 from its ideal location depends on the core/cladding offset of the GI fiber and the geometries of the dual-core fiber. The coupling efficiency also is affected by factors such as imperfections in index profile of the GI fiber, splicing induced deformation and the reflectance of the coating at the end face.

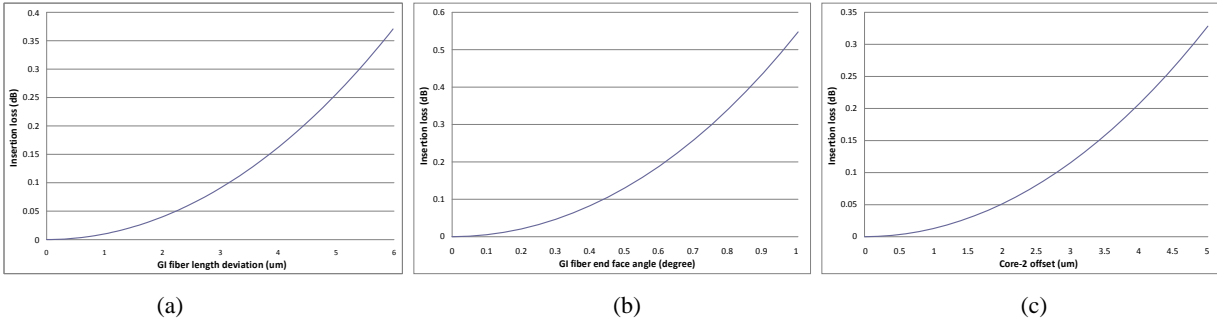


Figure 5. Loss of the turn-around vs. (a) deviation of the GI fiber length from the $\frac{1}{4}$ pitch length; (b) GI fiber end face cleave angle; and (c) offset of Core 2 from its ideal location.

The end face of the GI fiber was coated with a high reflection coating with a working temperature up to $300 \text{ }^\circ\text{C}$. To measure the loss of the turn-around, a piece of turn-around was spliced to a dual-core fiber. The spectral loss was then measured by the cutback method and is plotted in Figure 6. We can see in the wavelength range of interest, around 1064 nm , the loss is $< 0.4\text{dB}$, confirming our calculations.

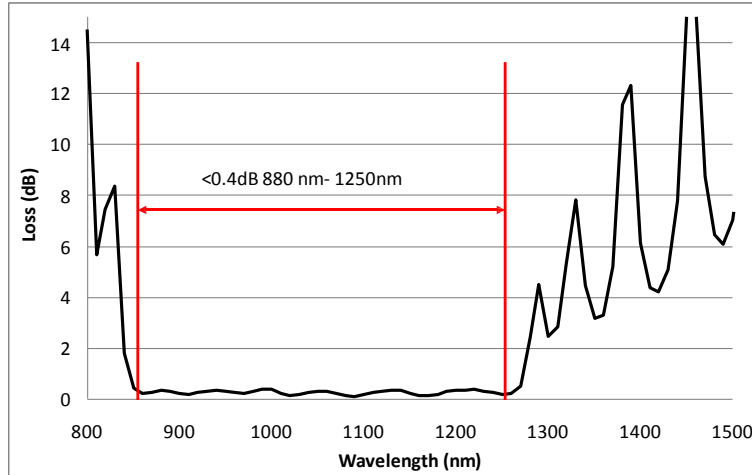


Figure 6. Spectral loss of the turn-around measured by the cutback method

3. CONCLUSION

In summary, we have experimentally demonstrated a miniature turn-around device using a dual-core fiber spliced to a graded index (GI) fiber lens. Since no section of the fiber is under bending stress or tension, the mechanical reliability is greatly improved, while cross-section and length are minimized. Furthermore, the device demonstrates low insertion loss over a wide wavelength range and is suitable for use in a dual-ended RDTS system.

4. ACKNOWLEDGEMENT

The authors would like to thank Paula Fournier for measuring the fiber and Deb Simoff for reviewing the manuscript.

REFERENCES

- [1] J. P. Dakin; D. J. Pratt; G. W. Bibby; J. N. Ross, "Distributed optical fiber Raman temperature sensor using a semiconductor light source and detector," *Electron. Lett.* **21**(13), 569–570 (1985).
- [2] K. Suh; C. Lee, "Auto-correction method for differential attenuation in a fiber-optic distributed-temperature sensor," *Opt. Lett.* **33**(16), 1845–1847 (2008).
- [3] Hwang, D.; Yoon, D.-J.; Kwon, I.-B.; Seo, D. C.; Chung, Y., "Novel auto-correction method in a fiber-optic distributed-temperature sensor using reflected anti-Stokes Raman scattering," *Optics Express*, **18**(10), 9747–9754 (2010).
- [4] Fernandez, A. F.; Rodeghiero, P.; Brichard, B.; Berghmans, F.; Hartog, A. H.; Hughes, P.; Williams, K.; Leach, A. P., "Radiation-tolerant Raman distributed temperature monitoring system for large nuclear infrastructures," *IEEE Transactions on Nuclear Science*, **52**(6), 2689–2694 (2005).
- [5] Bahaa E. A. Saleh, Malvin Carl Teich, [Fundamentals of Photonics], Wiley-Interscience, 18-23 (2007)
- [6] Frederick C. Allard, [Fiber Optics Handbook for Engineers and Scientists (Optical and Electro-Optical Engineering Series)], McGraw-Hill Publishing Companies, 3.6-3.10 (1990).